Bi-allelic *TARS* Mutations Are Associated with Brittle Hair Phenotype

Arjan F. Theil,[1,12] Elena Botta,[2,12] Anja Raams,[1] Desiree E.C. Smith,[3] Marisa I. Mendes,[3] Giuseppina Caligiuri,[2] Sarah Giachetti,[2] Silvia Bione,[2] Roberta Carriero,[2] Giordano Liberi,[2] Luca Zardoni,[2] Sigrid M.A. Swagemakers,[4] Gajja S. Salomons,[3,5] Alain Sarasin,[6] Alan Lehmann,[7] Peter J. van der Spek,[4] Tomoo Ogi,[8,9] Jan H.J. Hoeijmakers,[1,10,11] Wim Vermeulen,[1,*] and Donata Orioli[2,*]

Brittle and "tiger-tail" hair is the diagnostic hallmark of trichothiodystrophy (TTD), a rare recessive disease associated with a wide spectrum of clinical features including ichthyosis, intellectual disability, decreased fertility, and short stature. As a result of premature abrogation of terminal differentiation, the hair is brittle and fragile and contains reduced cysteine content. Hypersensitivity to UV light is found in about half of individuals with TTD; all of these individuals harbor bi-allelic mutations in components of the basal transcription factor TFIIH, and these mutations lead to impaired nucleotide excision repair and basal transcription. Different genes have been found to be associated with non-photosensitive TTD (NPS-TTD); these include *MPLKIP* (also called *TTDN1*), *GTF2E2* (also called *TFIIEβ*), and *RNF113A*. However, a relatively large group of these individuals with NPS-TTD have remained genetically uncharacterized. Here we present the identification of an NPS-TTD-associated gene, threonyl-tRNA synthetase (*TARS*), found by next-generation sequencing of a group of uncharacterized individuals with NPS-TTD. One individual has compound heterozygous *TARS* variants, c.826A>G (p.Lys276Glu) and c.1912C>T (p.Arg638*), whereas a second individual is homozygous for the *TARS* variant: c.680T>C (p.Leu227Pro). We showed that these variants have a profound effect on TARS protein stability and enzymatic function. Our results expand the spectrum of genes involved in TTD to include genes implicated in amino acid charging of tRNA, which is required for the last step in gene expression, namely protein translation. We previously proposed that some of the TTD-specific features derive from subtle transcription defects as a consequence of unstable transcription factors. We now extend the definition of TTD from a transcription syndrome to a "gene-expression" syndrome.

The multisystem neuroectodermal disease trichothiodystrophy (TTD) is a rare recessive genetic trait whose diagnostic hallmark is brittle hair.[1] The sparse and fragile hair is characterized by its typical "tiger-tail" banding pattern, which is seen when the hair is examined under a polarized light microscope; this pattern is associated with low cysteine content. Individuals with TTD express a wide and heterogeneous range of additional clinical features affecting multiple organs and tissues.[2] These features include ichthyosis, brittle nails, impaired intelligence, decreased fertility, short stature, anemia, and recurrent infections. Approximately 50% of individuals with TTD exhibit additional clinical and cellular photosensitivity. All of these photosensitive individuals with TTD (PS-TTD [MIM: 601675, 606390, 616395]) have bi-allelic mutations within the excision repair cross-complementation group 2 (*ERCC2* also called *XPD*; MIM: 126340]) gene,[3] the excision repair cross-complementation group 3 (*ERCC3* also called *XPB*; MIM: 133510]) gene,[4] or the general transcription factor II H, polypeptide 5 (*GTF2H5* also called *TTDA*; MIM: 608780]) gene.[5–7] These three genes encode for distinct subunits of the basal transcription factor IIH (TFIIH). In addition to its essential role in transcription initiation, TFIIH is also pivotal for nucleotide excision repair (NER), the sole DNA repair process in mammals that is able to remove DNA lesions induced by UV light (which is present in sunlight);[8] this explains the photosensitive phenotype. The dual function of TFIIH led to the hypothesis that part of the additional TTD features derive from tissue-specific impairments of transcription.[9–13] Indeed, reduced expression of tissue-specific genes has been observed in primary cells from individuals with TTD[14,15] as well as in neuronal cells or terminally differentiated keratinocytes derived from an *Ercc2* mutant mouse model that carries a single amino acid missense TTD-specific point mutation.[16,17] Importantly, TTD-associated pathogenic mutations cause severe instability of the mutant protein itself as well as the entire TFIIH complex in which they reside, resulting in reduced steady-state protein amounts in subject-derived primary fibroblasts.[18–20] In addition, we previously identified a thermo-labile single amino acid missense mutation in *ERCC2* in an individual

[1]Department of Molecular Genetics, Oncode Institute, Erasmus University Medical Center, University Medical Center Rotterdam, 3015 GD Rotterdam, the Netherlands; [2]Istituto di Genetica Molecolare, Consiglio Nazionale delle Ricerche, 27100 Pavia, Italy; [3]Metabolic Unit, Department of Clinical Chemistry, Amsterdam University Medical Center and Amsterdam Gastroenterology and Metabolism, Vrije Universiteit Amsterdam, Amsterdam Neuroscience, 1081 HZ Amsterdam, the Netherlands; [4]Department of Pathology and Clinical Bioinformatics Unit, Erasmus University Medical Center, 3015 GD Rotterdam, the Netherlands; [5]Genetic Metabolic Diseases, Amsterdam University Medical Center, University of Amsterdam, 1081 HZ Amsterdam, the Netherlands; [6]Institut Gustave Roussy, UMR8200 CNRS, 94805 Villejuif, France; [7]Genome Damage and Stability Centre, School of Life Sciences, University of Sussex, Falmer, Brighton BN1 9RH, UK; [8]Department of Genetics, Research Institute of Environmental Medicine, Nagoya University, Nagoya, Japan; [9]Department of Human Genetics and Molecular Biology, Graduate School of Medicine, Nagoya University, Nagoya 464-0805, Japan; [10]Princess Maxima Center for Pediatric Oncology, Oncode Institute, 3584 CS Utrecht, the Netherlands; [11]CECAD Forschungszentrum, University of Cologne, 50931 Cologne, Germany
[12]These authors contributed equally to this work
*Correspondence: w.vermeulen@erasmusmc.nl (W.V.), orioli@igm.cnr.it (D.O.)
https://doi.org/10.1016/j.ajhg.2019.06.017.

with mild TTD. We found a strong decline in the total TFIIH amount, repair capacity, and transcription levels upon culturing subject-derived fibroblasts at slightly elevated temperatures; this mimics the striking aggravation of TTD-specific features this individual has experienced after episodes of fever.[11] These findings further corroborate the idea that some of the TTD-associated transcription defects are derived from transcription factor instability. The other half of the TTD-affected individuals who were studied are non-photosensitive and NER-proficient. The non-photosensitive TTD (NPS-TTD [MIM: 234050, 616943, 300953]) in these individuals is caused by mutations in *MPLKIP* (also called *TTDN1*; MIM: 609188);[21,22] in *GTF2E2* (also called *TFIIEβ*; MIM: 189964);[23,24] in the only X-linked TTD-associated gene, *RNF113A* (OMIM: 300951); [25] or in an as-yet-unidentified gene or genes.

Strikingly, a strong reduction of the total amount of both subunits of the transcription initiation factor TFIIE was observed in primary fibroblasts of *GTF2E2*-mutated subjects, but this reduction nevertheless did not significantly affect the overall basal transcription capacity. However, these mutations caused reduced TFIIH-mediated phosphorylation of the TFIIEα subunit.[23] Induced pluripotent stem cell (iPS) reprogramming of these fibroblasts and subsequent *in vitro* differentiation into a red blood cell lineage revealed a hematopoietic defect during late-stage differentiation; this defect is associated with hemoglobin subunit imbalance, recapitulating the subjects' anemia.[24,26] In these differentiated cells, fragile TFIIE becomes limited in its ability to efficiently support transcription of globin genes. Hemoglobin subunit imbalance is commonly induced by impaired transcription, thus corroborating the idea that some of the typical TTD-features are not only due to altered transcription but may also be further aggravated by unstable transcription factors. Recently, the biological function of another NPS-TTD-associated protein, RNF113A, was identified and shown to be associated with the splicing machinery.[27] This observation seems to broaden the hypothesis that, in addition to transcription initiation impairments, TTD features may also be caused by mRNA processing alterations. Currently, many individuals with NPS-TTD are still genetically uncharacterized, so there is potential for expanding the spectrum of possible TTD-associated genes. Discovering additional NPS-TTD-associated genes will further increase our understanding of how gene expression defects cause TTD-associated phenotypes.

To identify disease-associated genes and the molecular basis of NPS-TTD, we performed whole-genome sequencing (WGS)[28,29] and whole-exome sequencing (WES) in a selected group of 24 unassigned individuals with NPS-TTD. Biological samples were obtained with appropriate informed consent and according to the protocols approved by institute-specific ethical review boards. Sequence data were aligned to the human reference genome and provided as lists of sequence variants (SNPs and short indels) relative to this reference genome. Analysis of the sequence variants revealed that two affected individuals were carriers of homozygous or compound-heterozygous variants within the threonyl-tRNA synthetase (*TARS* [MIM: 187790]) gene (GenBank: NM_152295.4 transcript variant 1 and GenBank: NP_689508.3). Subject TTD18PV was born in 1990 to non-consanguineous Italian parents and clinically diagnosed with TTD in 1992 on the basis of hair analysis, which revealed that hairs from this individual had lower cysteine content (8.5%) than did hairs from healthy donors (20.8%). Intriguingly, a significantly lower level of the amino acid threonine (Thr) was also found in this individual's hair (3% compared to 6.9% in hair from healthy donors), which was not observed for any other amino acid (Table S1). The hair showed fractures (trichoschisis) and the typical, for TTD, appearance of an alternating light and dark banding pattern ("tiger tail") when analyzed under polarization microscopy. There were no signs of sun-sensitive skin, but ichthyosis and follicular keratosis were reported. Additional associated features were delayed physical development, recurrent infections of the respiratory tract, and acromandibular dysplasia. No later records exist for this individual. Two allelic *TARS* variants, c.826A>G (p.Lys276Glu) and c.1912C>T (p.Arg638*) (GenBank NM_152295.4) were identified in this individual (Figure 1). Subject TTD5VI was also clinically diagnosed with TTD based on hair analysis, which revealed an abnormal structure of the hair shaft both visually and under the microscope ("tiger-tail" banding pattern). She was born encased in a tight, shiny membrane ("collodion baby") and had ichthyosis, both commonly associated with TTD.[2] Also for this case, no follow-up clinical report is available. In subject TTD5VI, we identified a homozygous variant within the *TARS* gene: c.680T>C (p.Leu227Pro]) (Figure 1) (GenBank: NM_152295.4). We confirmed the absence of DNA repair deficiency by assessing the UV-irradiation sensitivity and the NER capacity; we did this through the use of clonogenic UV-survival and unscheduled DNA-repair synthesis assays, respectively (Figure S1). The presence of all three *TARS* variants was confirmed by Sanger sequencing (Figure 1A). The missense variant c.826A>G (p.Lys276Glu) is not present in public databases, and it obtained high pathogenicity scores in three prediction algorithms (PolyPhen-2 score 0.763 = possibly damaging; Mutation Taster score = disease causing with $p = 0.999$; CADD_phred score = 25.7). The nonsense variant c.1912C>T is reported in the ExAC database but only in the heterozygous condition (allele frequency = 0.00008661). The missense variant c.680T>C (p.Leu227Pro) in TTD5VI is also not present in public databases, and it obtained high pathogenicity scores in three prediction algorithms (PolyPhen-2 score 0.994 = damaging; Mutation Taster score = disease causing with $p = 1$; CADD_phred score = 32). All three variants are thus predicted to be pathogenic and to produce either a C-terminal truncated TARS protein (in case of p.Arg638*) or an amino acid substitution in a highly conserved residue (in the cases of p.Leu227Pro and p.Lys276Glu) (Figure 1B). After identification of the *TARS* mutations in TTD18PV and TTD5VI, we performed Sanger

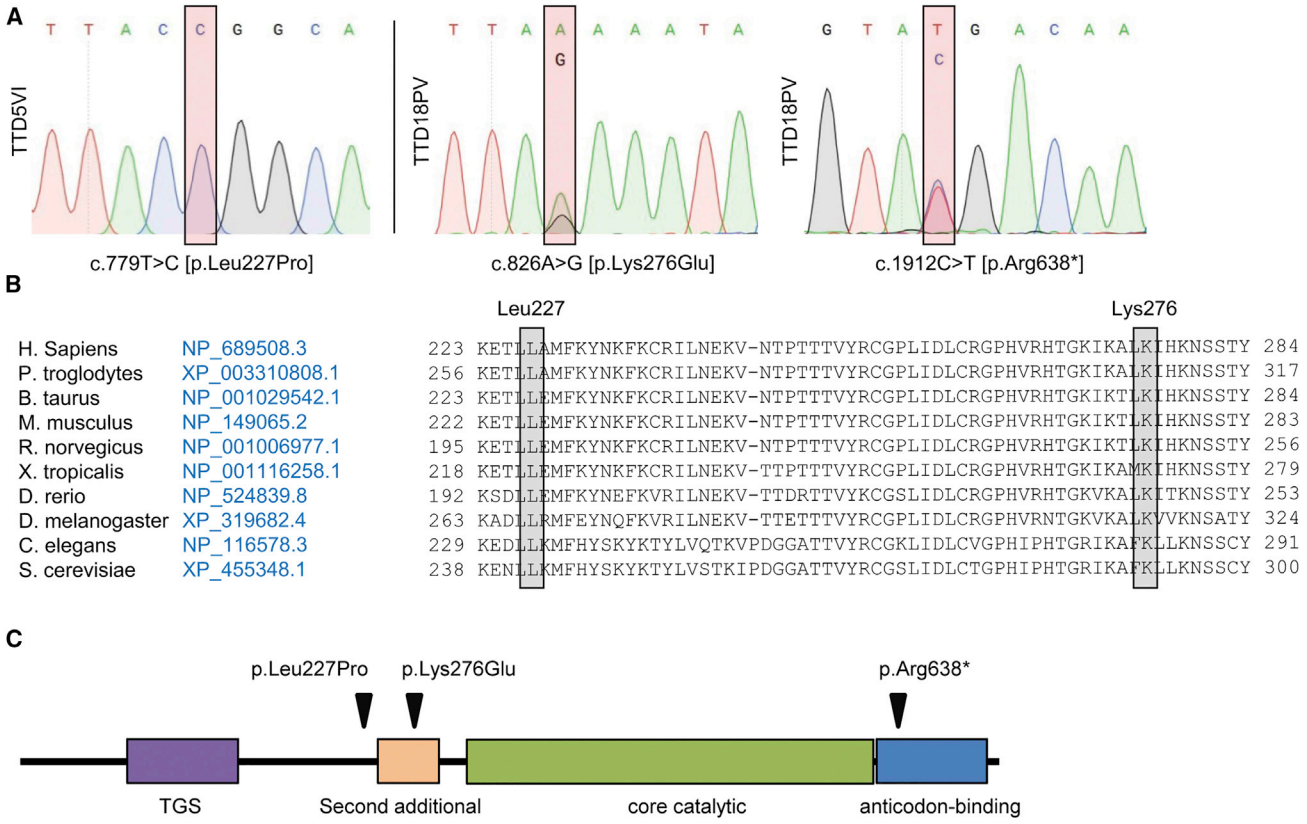

Figure 1. Identification of *TARS* Variants
(A) Sanger sequencing profiles of *TARS* cDNA. Subject TTD5VI shows homozygosity for the c.680T>C missense variant (right panel), and subject TTD18PV shows compound heterozygosity for missense variant c.826A>G (left panel) and nonsense variant c.1912C>T (middle panel).
(B) Amino acid conservation across different species orthologs.
(C) Schematic representation (created with InterPro) of the domain structure of the TARS protein with the location of the subjects' variants.

sequencing of *TARS* cDNA in 24 additional individuals with unsolved NPS-TTD. No bi-allelic mutations were identified. This indicates that in our combined cohort of 47 affected individuals (17 cases in the Dutch cohort; 16 cases from 14 families in the Italian cohort; 16 cases in the UK cohort), defective *TARS* accounts for about 4% of individuals with NPS-TTD.

TARS is an essential component of the translation machinery, and it belongs to the aminoacyl-tRNA synthetase (ARS) protein family.[30,31] This family is divided into two subgroups, class I and class II ARS proteins, based on their structure and presence of shared functional domains.[32–34] TARS is a class II ARS protein and catalyzes the covalent binding of threonine to a threonine-specific tRNA ($tRNA^{Thr}$) to form the aminoacyl Thr-$tRNA^{Thr}$ complex.[35,36] The inactive monomeric form of TARS needs to dimerize first in order to establish a catalytically active configuration, which allows specific binding of each monomer to the corresponding uncharged tRNA and free amino acid Thr. Amino acid charging is highly specific and facilitated by several conserved domains within TARS (Figure 1C) that include the C-terminal anticodon-binding domain, the catalytic core domain, a putative N-terminal editing domain, a mode of the so-called second additional domain, and a structurally uncharacterized TGS (for ThrRS, GTPase, and SpoT) domain. The second additional domain consists of several antiparallel beta sheets that surround the dimeric and catalytically active core, whereas the TGS domain appears to facilitate nucleotide binding.[36] The identified amino acid substitutions in subjects TTD18PV and TTD5VI are close to the core catalytic domain and might have an impact on the catalytic activity of the protein.

Immunoblot analysis of whole-cell extracts from TTD18PV and TTD5VI subject fibroblasts revealed a strong reduction in the total cellular amount of full-length TARS in both subjects' lysates (to approximately 20% of the amount seen in controls) (Figure 2A and 2B). The TARS-specific protein bands were of the same molecular mass as that seen in control lysates, and this mass corresponded to the predicted protein mass containing the amino substitutions p.Lys276Glu or p.Leu227Pro (Figure 2A and 2B). The TARS variant c.1912C>T (p.Arg638*) is predicted to lack the last 85 amino acid residues at the C-terminal end; this would almost completely delete the anticodon binding domain. However, this predicted lower-sized

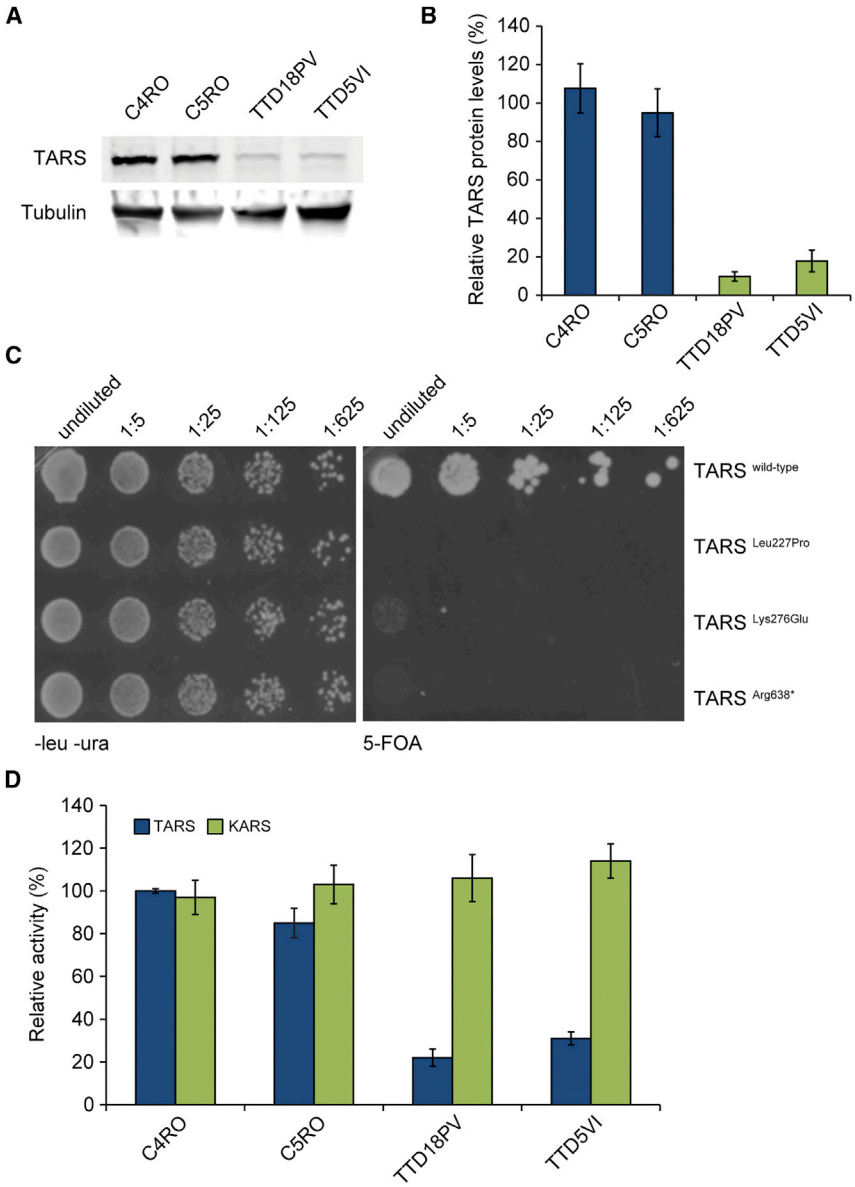

Figure 2. Functional Consequence of *TARS* Variants

(A) Immunoblot analysis used for determining TARS protein amounts in lysates of primary fibroblasts TTD5VI and TTD18PV and two wild-type controls; anti-tubulin was used as a loading control.

(B) Quantification of the immunoblot. The band intensities of TARS were normalized to tubulin and expressed as percentage of the intensities for control cells (C4RO). The error bars indicate the SEM of three independent experiments.

(C) Representative picture of a yeast complementation assay. Wild-type and mutant strains were grown on solid medium without leucine and uracil (−LU; left panels) or in the presence of 5-FOA (right panels). Cells were spotted with serial dilutions and pictures were taken after 96 h at 30°C.

(D) The cytosolic fraction from TTD5VI, TTD18PV, and two control fibroblasts was used for determining TARS (blue) and KARS (green; internal control) amino acid charging on tRNA. Threonine and lysine charging in control fibroblast C4RO was set at 100%, and error bars indicate SD of three independent experiments.

protein band was not visible in immunoblots, indicating that this mutant protein might be less abundantly synthetized and/or severely unstable as a result of the C-terminal truncation. Total *TARS* mRNA levels, as measured by real-time quantitative reverse-transcription PCR (qRT-PCR), were only slightly reduced in TTD18PV primary fibroblasts compared to control cells (Figure S2). Allele-specific qRT-PCR showed that only ~10% of the total *TARS* mRNA molecules in TTD18PV primary fibroblasts originated from the c.1912C>T variant allele, suggesting that in TTD18PV, most TARS proteins contain the missense Lys276Glu TARS variant. Altogether, these data show that the single amino acid substitutions p.Leu227Pro and p.Lys276Glu in TARS cause severe protein instability.

Next, we tested the functionality of the identified TARS variants by using a well-established complementation yeast assay.[37] It has been recently demonstrated that the haploid yeast knockout *Saccharomyces cerevisiae* strain deprived of the *TARS* ortholog *THS1* essential gene (Δths1) can be complemented by the human *TARS* cDNA.[38] We could therefore use plasmid shuffling experiments to test the ability of c.680T>C (p.Leu227Pro), c.826A>G (p.Lys276Glu), and c.1912C>T (p.Arg638*) variants to rescue the cell lethality associated with the deletion of the endogenous yeast *THS1*. In comparison with those expressing wild-type *TARS*, yeast cells expressing the variants showed dramatically reduced growth, strongly supporting the notion that these protein alterations severely impact TARS functionality (Figure 2C).

To further investigate the functional consequences of the *TARS* variants in the context of mammalian cells, we measured steady-state aminoacylation reactions on protein lysates from subjects' fibroblasts (from TTD5VI and TTD18PV) and control fibroblasts (from C4RO and C5RO). KARS (for Lysine-tRNA synthetase) activity was simultaneously measured as an internal control. Intra-assay variation was <15%, and no decreases were observed for KARS (internal control) activity. In contrast, the results showed an approximate 70%–80% reduction of threonine tRNA charging activity in both subject cells as compared to control fibroblasts (Figure 2D). These data corroborate the results obtained from the yeast-based complementation assays and demonstrate the loss-of-function (LoF) effect of *TARS* variants on tRNA charging activity.

In summary, we identified bi-allelic *TARS* variants affecting highly conserved amino acids in two unrelated individuals with NPS-TTD (Figures 1A and 1B): compound-heterozygous variants in subject TTD18PV (c.826A>G [p.Lys276Glu] and c.1912C>T [p.Arg638*]), and a homozygous variant in subject TTD5VI (c.680T>C [p.Leu227Pro]). Immunoblotting revealed an approximately 80% reduction of steady-state protein amounts of full-length TARS in fibroblast lysates from subjects TTD18PV and TTD5VI when these cells were compared to control fibroblasts. We are tempted to speculate that the identified amino acid substitutions compromise the structural integrity of the dimeric and catalytically active TARS complex and perhaps force the dimeric TARS protein complex into its monomeric and inactive form, which might be unstable and more susceptible to protein degradation. Protein instability seems to be a common cellular hallmark observed in TTD cells; it was also observed for TTD-subject cells carrying mutations in either TFIIH (*ERCC3*, *ERCC2*, or *TFB5/TTD* [also called *TTDA*]) or TFIIE (*GTF2E2*).[7,11,19,20,23,24,39]

The canonical function of TARS in tRNA charging strongly depends on its structural conformation and correct assembly of a catalytically active dimeric TARS complex. It is thus likely that along with haploinsufficiency caused by protein instability the catalytic activity of mutant TARS is also affected, and this contributes to the phenotype. The lack of complementation in yeast strains overexpressing the missense TARS variants (Figure 2C) supports this hypothesis. This reduced activity will decrease the number of charged $tRNA^{Thr}$ molecules available for translation in subjects' cells, impairing protein production in general. However, it is important to understand the degree to which translation is impaired and contributes to tissue-specific phenotypes. There is also evidence suggesting that proofreading deficiencies might increase the number of mischarged tRNA molecules, and such an increase might lead to accumulation of misfolded proteins in the brain and thus cause progressive neurological phenotypes.[40]

Bi-allelic mutations in other ARS-related genes typically cause severe, early-onset, recessive diseases that affect a wide range of tissues.[41] The vast majority of these bi-allelic mutations also show LoF effects, reduction in ARS protein amounts,[41,42] and severe decreases in enzyme activity. Mutations in *TARS* have not yet been associated with human disorders. The notion that *TARS* variants are associated with clinical features such as brittle hair and ichthyosis is somewhat surprising because ARS-mediated LoF effects were thus far not linked to brittle hair or ichthyosis.[43] However, very recently, inactivation mutations in the cysteinyl-tRNA synthetase (*CARS* [MIM: 123859]) have been identified in three unrelated families with wide clinical spectra and some TTD-phenotype-reminiscent features, including microcephaly, developmental delay, and brittle hair with weak or moderate "tiger-tail" banding.[44] The few cases identified so far do not allow one to determine whether the clinical differences between TARS- and CARS-defective individuals are due to the type of mutations or to the impact that alterations in specific ARSs may have on cellular metabolism.

The notion that faulty tRNA charging, which would likely reduce protein translation, is associated with TTD-specific features suggests that gene expression defects (i.e., the net result of transcription, transcript maturation and stability, and protein synthesis and stability) comprise the underlying molecular mechanism that drives segmental TTD features. Our observation that TTD is also associated with affected protein translation, together with the notion that another TTD-causing mutation was found in an mRNA splicing factor,[27] prompted us to extend the definition of TTD from being a transcription syndrome to a gene-expression syndrome.

This expanding spectrum of TTD-associated genes will contribute to a better understanding of the molecular mechanisms underlying the rare genetic disorder TTD. Besides known impairments in genome maintenance and transcription failure, anomalies in translation also appear to contribute to TTD-specific clinical features such as brittle hair.

Supplemental Data

Supplemental Data can be found online at https://doi.org/10.1016/j.ajhg.2019.06.017.

Acknowledgments

This work was supported by grants from Associazione Italiana Ricerca sul Cancro (17710 and 21737) to D.O., from the Telethon Foundation (GEP13022) to E.B., from the European Research Council (ERC; grant number 233424) to J.H., and from the Dutch Science Organization (NWO) ZonMW division (grant number 912.12.132) and the European Research Council (ERC; grant number 340988) to W.V. We thank the Optical Imaging Centre (OIC) of the Erasmus University Medical Center for microscopy support and Xiao-Long Zhou (Institute of Biochemistry and Cell Biology, Shanghai Institutes for Biological Sciences, Shanghai, China) for providing the Δths1 yeast strain and TARS expressing vectors. The bioinformatics work was financially supported by an H2020 grant (BigMedilytics, big data for medical analysis). We would like to thank Joost Verlouw, Pascal Arp, and Mila Jhamai for help with WES and variant calling.

Declaration of Interests

The authors declare no competing interests.

Received: March 28, 2019
Accepted: June 24, 2019
Published: August 1, 2019

Web Resources

Alamut Visual, https://www.interactive-biosoftware.com/alamut-visual/
ANNOVAR, http://annovar.openbioinformatics.org/en/latest/
Complete Genomics, https://www.completegenomics.com/sequence-data/cgatools/
dbSNP, https://www.ncbi.nlm.nih.gov/projects/SNP/

GenBank, https://www.ncbi.nlm.nih.gov/genbank/
Human Genome Variation Society, http://www.hgvs.org/mutnomen/
Illumina, https://www.illumina.com/
Ingenuity Variant Analysis, https://www.ingenuity.com/products/variant-analysis
Interpro, https://www.ebi.ac.uk/interpro/
MutationTaster, http://www.mutationtaster.org/
NCBI HomoloGene, https://www.ncbi.nlm.nih.gov/homologene
PolyPhen-2, http://genetics.bwh.harvard.edu/pph2/
OMIM, https://www.omim.org/
RefSeq, http://www.ncbi.nlm.nih.gov/RefSeq
Sequence Variant Nomenclature, http://varnomen.hgvs.org/

References

1. Price, V.H., Odom, R.B., Ward, W.H., and Jones, F.T. (1980). Trichothiodystrophy: sulfur-deficient brittle hair as a marker for a neuroectodermal symptom complex. Arch. Dermatol. *116*, 1375–1384.
2. Faghri, S., Tamura, D., Kraemer, K.H., and Digiovanna, J.J. (2008). Trichothiodystrophy: a systematic review of 112 published cases characterises a wide spectrum of clinical manifestations. J. Med. Genet. *45*, 609–621.
3. Stefanini, M., Lagomarsini, P., Arlett, C.F., Marinoni, S., Borrone, C., Crovato, F., Trevisan, G., Cordone, G., and Nuzzo, F. (1986). Xeroderma pigmentosum (complementation group D) mutation is present in patients affected by trichothiodystrophy with photosensitivity. Hum. Genet. *74*, 107–112.
4. Weeda, G., Rossignol, M., Fraser, R.A., Winkler, G.S., Vermeulen, W., van 't Veer, L.J., Ma, L., Hoeijmakers, J.H., and Egly, J.M. (1997). The XPB subunit of repair/transcription factor TFIIH directly interacts with SUG1, a subunit of the 26S proteasome and putative transcription factor. Nucleic Acids Res. *25*, 2274–2283.
5. Giglia-Mari, G., Coin, F., Ranish, J.A., Hoogstraten, D., Theil, A., Wijgers, N., Jaspers, N.G., Raams, A., Argentini, M., van der Spek, P.J., et al. (2004). A new, tenth subunit of TFIIH is responsible for the DNA repair syndrome trichothiodystrophy group A. Nat. Genet. *36*, 714–719.
6. Stefanini, M., Botta, E., Lanzafame, M., and Orioli, D. (2010). Trichothiodystrophy: From basic mechanisms to clinical implications. DNA Repair (Amst.) *9*, 2–10.
7. Theil, A.F., Hoeijmakers, J.H., and Vermeulen, W. (2014). TTDA: Big impact of a small protein. Exp. Cell Res. *329*, 61–68.
8. Marteijn, J.A., Lans, H., Vermeulen, W., and Hoeijmakers, J.H. (2014). Understanding nucleotide excision repair and its roles in cancer and ageing. Nat. Rev. Mol. Cell Biol. *15*, 465–481.
9. Vermeulen, W., van Vuuren, A.J., Chipoulet, M., Schaeffer, L., Appeldoorn, E., Weeda, G., Jaspers, N.G., Priestley, A., Arlett, C.F., Lehmann, A.R., et al. (1994). Three unusual repair deficiencies associated with transcription factor BTF2(TFIIH): Evidence for the existence of a transcription syndrome. Cold Spring Harb. Symp. Quant. Biol. *59*, 317–329.
10. Bergmann, E., and Egly, J.M. (2001). Trichothiodystrophy, a transcription syndrome. Trends Genet. *17*, 279–286.
11. Vermeulen, W., Rademakers, S., Jaspers, N.G., Appeldoorn, E., Raams, A., Klein, B., Kleijer, W.J., Hansen, L.K., and Hoeijmakers, J.H. (2001). A temperature-sensitive disorder in basal transcription and DNA repair in humans. Nat. Genet. *27*, 299–303.
12. Dubaele, S., Proietti De Santis, L., Bienstock, R.J., Keriel, A., Stefanini, M., Van Houten, B., and Egly, J.M. (2003). Basal transcription defect discriminates between xeroderma pigmentosum and trichothiodystrophy in XPD patients. Mol. Cell *11*, 1635–1646.
13. Keriel, A., Stary, A., Sarasin, A., Rochette-Egly, C., and Egly, J.M. (2002). XPD mutations prevent TFIIH-dependent transactivation by nuclear receptors and phosphorylation of RARalpha. Cell *109*, 125–135.
14. Orioli, D., Compe, E., Nardo, T., Mura, M., Giraudon, C., Botta, E., Arrigoni, L., Peverali, F.A., Egly, J.M., and Stefanini, M. (2013). XPD mutations in trichothiodystrophy hamper collagen VI expression and reveal a role of TFIIH in transcription derepression. Hum. Mol. Genet. *22*, 1061–1073.
15. Arseni, L., Lanzafame, M., Compe, E., Fortugno, P., Afonso-Barroso, A., Peverali, F.A., Lehmann, A.R., Zambruno, G., Egly, J.M., Stefanini, M., and Orioli, D. (2015). TFIIH-dependent MMP-1 overexpression in trichothiodystrophy leads to extracellular matrix alterations in patient skin. Proc. Natl. Acad. Sci. USA *112*, 1499–1504.
16. de Boer, J., de Wit, J., van Steeg, H., Berg, R.J., Morreau, H., Visser, P., Lehmann, A.R., Duran, M., Hoeijmakers, J.H., and Weeda, G. (1998). A mouse model for the basal transcription/DNA repair syndrome trichothiodystrophy. Mol. Cell *1*, 981–990.
17. Compe, E., Malerba, M., Soler, L., Marescaux, J., Borrelli, E., and Egly, J.M. (2007). Neurological defects in trichothiodystrophy reveal a coactivator function of TFIIH. Nat. Neurosci. *10*, 1414–1422.
18. Theil, A.F., Nonnekens, J., Steurer, B., Mari, P.O., de Wit, J., Lemaitre, C., Marteijn, J.A., Raams, A., Maas, A., Vermeij, M., et al. (2013). Disruption of TTDA results in complete nucleotide excision repair deficiency and embryonic lethality. PLoS Genet. *9*, e1003431.
19. Botta, E., Nardo, T., Lehmann, A.R., Egly, J.M., Pedrini, A.M., and Stefanini, M. (2002). Reduced level of the repair/transcription factor TFIIH in trichothiodystrophy. Hum. Mol. Genet. *11*, 2919–2928.
20. Vermeulen, W., Bergmann, E., Auriol, J., Rademakers, S., Frit, P., Appeldoorn, E., Hoeijmakers, J.H., and Egly, J.M. (2000). Sublimiting concentration of TFIIH transcription/DNA repair factor causes TTD-A trichothiodystrophy disorder. Nat. Genet. *26*, 307–313.
21. Botta, E., Offman, J., Nardo, T., Ricotti, R., Zambruno, G., Sansone, D., Balestri, P., Raams, A., Kleijer, W.J., Jaspers, N.G., et al. (2007). Mutations in the C7orf11 (TTDN1) gene in six nonphotosensitive trichothiodystrophy patients: No obvious genotype-phenotype relationships. Hum. Mutat. *28*, 92–96.
22. Heller, E.R., Khan, S.G., Kuschal, C., Tamura, D., DiGiovanna, J.J., and Kraemer, K.H. (2015). Mutations in the TTDN1 gene are associated with a distinct trichothiodystrophy phenotype. J. Invest. Dermatol. *135*, 734–741.
23. Kuschal, C., Botta, E., Orioli, D., Digiovanna, J.J., Seneca, S., Keymolen, K., Tamura, D., Heller, E., Khan, S.G., Caligiuri, G., et al. (2016). GTF2E2 mutations destabilize the general transcription factor complex TFIIE in individuals with DNA repair-proficient trichothiodystrophy. Am. J. Hum. Genet. *98*, 627–642.
24. Theil, A.F., Mandemaker, I.K., van den Akker, E., Swagemakers, S.M.A., Raams, A., Wüst, T., Marteijn, J.A., Giltay, J.C., Colombijn, R.M., Moog, U., et al. (2017). Trichothiodystrophy causative TFIIEβ mutation affects transcription in highly differentiated tissue. Hum. Mol. Genet. *26*, 4689–4698.

25. Corbett, M.A., Dudding-Byth, T., Crock, P.A., Botta, E., Christie, L.M., Nardo, T., Caligiuri, G., Hobson, L., Boyle, J., Mansour, A., et al. (2015). A novel X-linked trichothiodystrophy associated with a nonsense mutation in RNF113A. J. Med. Genet. *52*, 269–274.
26. Viprakasit, V., Gibbons, R.J., Broughton, B.C., Tolmie, J.L., Brown, D., Lunt, P., Winter, R.M., Marinoni, S., Stefanini, M., Brueton, L., et al. (2001). Mutations in the general transcription factor TFIIH result in beta-thalassaemia in individuals with trichothiodystrophy. Hum. Mol. Genet. *10*, 2797–2802.
27. Wu, N.Y., Chung, C.S., and Cheng, S.C. (2017). Role of Cwc24 in the first catalytic step of splicing and fidelity of 5′ splice site selection. Mol. Cell. Biol. *37*, e00580–e16.
28. Drmanac, R., Sparks, A.B., Callow, M.J., Halpern, A.L., Burns, N.L., Kermani, B.G., Carnevali, P., Nazarenko, I., Nilsen, G.B., Yeung, G., et al. (2010). Human genome sequencing using unchained base reads on self-assembling DNA nanoarrays. Science *327*, 78–81.
29. Swagemakers, S.M., Jaspers, N.G., Raams, A., Heijsman, D., Vermeulen, W., Troelstra, C., Kremer, A., Lincoln, S.E., Tearle, R., Hoeijmakers, J.H., and van der Spek, P.J. (2014). Pollitt syndrome patients carry mutation in TTDN1. Meta Gene *2*, 616–618.
30. Ibba, M., and Soll, D. (2000). Aminoacyl-tRNA synthesis. Annu. Rev. Biochem. *69*, 617–650.
31. Rajendran, V., Kalita, P., Shukla, H., Kumar, A., and Tripathi, T. (2018). Aminoacyl-tRNA synthetases: Structure, function, and drug discovery. Int. J. Biol. Macromol. *111*, 400–414.
32. Bryson, D.I., Fan, C., Guo, L.T., Miller, C., Söll, D., and Liu, D.R. (2017). Continuous directed evolution of aminoacyl-tRNA synthetases. Nat. Chem. Biol. *13*, 1253–1260.
33. Chaliotis, A., Vlastaridis, P., Mossialos, D., Ibba, M., Becker, H.D., Stathopoulos, C., and Amoutzias, G.D. (2017). The complex evolutionary history of aminoacyl-tRNA synthetases. Nucleic Acids Res. *45*, 1059–1068.
34. Eriani, G., Delarue, M., Poch, O., Gangloff, J., and Moras, D. (1990). Partition of tRNA synthetases into two classes based on mutually exclusive sets of sequence motifs. Nature *347*, 203–206.
35. Smith, T.F., and Hartman, H. (2015). The evolution of class II aminoacyl-tRNA synthetases and the first code. FEBS Lett. *589*, 3499–3507.
36. Sankaranarayanan, R., Dock-Bregeon, A.C., Romby, P., Caillet, J., Springer, M., Rees, B., Ehresmann, C., Ehresmann, B., and Moras, D. (1999). The structure of threonyl-tRNA synthetase-tRNA(Thr) complex enlightens its repressor activity and reveals an essential zinc ion in the active site. Cell *97*, 371–381.
37. Oprescu, S.N., Griffin, L.B., Beg, A.A., and Antonellis, A. (2017). Predicting the pathogenicity of aminoacyl-tRNA synthetase mutations. Methods *113*, 139–151.
38. Ruan, Z.R., Fang, Z.P., Ye, Q., Lei, H.Y., Eriani, G., Zhou, X.L., and Wang, E.D. (2015). Identification of lethal mutations in yeast threonyl-tRNA synthetase revealing critical residues in its human homolog. J. Biol. Chem. *290*, 1664–1678.
39. Botta, E., Nardo, T., Orioli, D., Guglielmino, R., Ricotti, R., Bondanza, S., Benedicenti, F., Zambruno, G., and Stefanini, M. (2009). Genotype-phenotype relationships in trichothiodystrophy patients with novel splicing mutations in the XPD gene. Hum. Mutat. *30*, 438–445.
40. Lee, J.W., Beebe, K., Nangle, L.A., Jang, J., Longo-Guess, C.M., Cook, S.A., Davisson, M.T., Sundberg, J.P., Schimmel, P., and Ackerman, S.L. (2006). Editing-defective tRNA synthetase causes protein misfolding and neurodegeneration. Nature *443*, 50–55.
41. Antonellis, A., Oprescu, S.N., Griffin, L.B., Heider, A., Amalfitano, A., and Innis, J.W. (2018). Compound heterozygosity for loss-of-function FARSB variants in a patient with classic features of recessive aminoacyl-tRNA synthetase-related disease. Hum. Mutat. *39*, 834–840.
42. Nakayama, T., Wu, J., Galvin-Parton, P., Weiss, J., Andriola, M.R., Hill, R.S., Vaughan, D.J., El-Quessny, M., Barry, B.J., Partlow, J.N., et al. (2017). Deficient activity of alanyl-tRNA synthetase underlies an autosomal recessive syndrome of progressive microcephaly, hypomyelination, and epileptic encephalopathy. Hum. Mutat. *38*, 1348–1354.
43. Meyer-Schuman, R., and Antonellis, A. (2017). Emerging mechanisms of aminoacyl-tRNA synthetase mutations in recessive and dominant human disease. Hum. Mol. Genet. *26* (R2), R114–R127.
44. Kuo, M.E., Theil, A.F., Kievit, A., Malicdan, M.C., Introne, W.J., Christian, T., Verheijen, F.W., Smith, D.E.C., Mendes, M.I., Hussaarts-Odijk, L., et al. (2019). Cysteinyl-tRNA synthetase mutations cause a multi-system, recessive disease that includes microcephaly, developmental delay, and brittle hair and nails. Am. J. Hum. Genet. *104*, 520–529.

The American Journal of Human Genetics, Volume *105*

Supplemental Data

Bi-allelic *TARS* Mutations Are Associated with Brittle Hair Phenotype

Arjan F. Theil, Elena Botta, Anja Raams, Desiree E.C. Smith, Marisa I. Mendes, Giuseppina Caligiuri, Sarah Giachetti, Silvia Bione, Roberta Carriero, Giordano Liberi, Luca Zardoni, Sigrid M.A. Swagemakers, Gajja S. Salomons, Alain Sarasin, Alan Lehmann, Peter J. van der Spek, Tomoo Ogi, Jan H.J. Hoeijmakers, Wim Vermeulen, and Donata Orioli

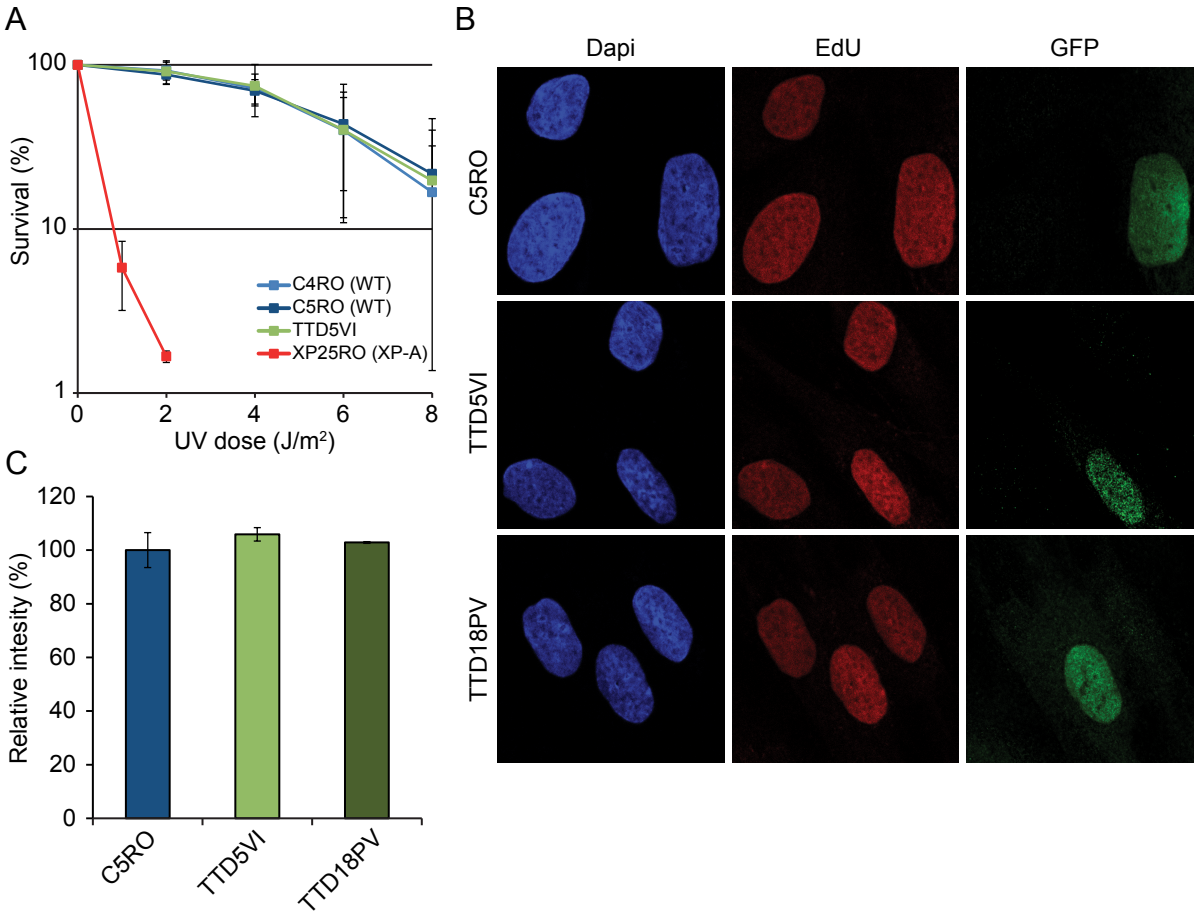

Figure S1. Characterization of DNA Repair capacity. (A) Clonogenic UV-survival assay to measure UV-sensitivity. One day after seeding of respectively TTD5VI, NER-defective XP-A (XP25RO) and NER-proficient fibroblasts (C4RO and C5RO), the cells were irradiated with the indicated (X-axis) doses of UV and cultures incubated for two weeks to grow colonies. Survival was plotted as the percentage of colonies obtained after treatment compared to the mean number of colonies from the mock-treated cells (set at 100%). The error bars indicate SEM of three independent experiments. (B) Global NER activities measured as UV-induced unscheduled DNA synthesis (UDS), using EdU incorporation after UV-irradiation, visualized by fluorescence-conjugated azide (Click-iT assay). Shown are representative pictures from the UDS experiment performed on primary fibroblasts of TTD5VI or TTD18PV and compared to NER-proficient (wild-type) control primary fibroblasts C5RO. To directly compare UDS levels with known NER-proficient cells, the wild-type fibroblasts that stably express GFP were mixed with the test cells. UDS-derived fluorescence is shown in red (middle panel) and nuclear staining in blue (DAPI)(left panel), NER-proficient cells can be distinguished by the GFP signal (green, right panel). (C) Quantification of the UDS experiments. Mean intensities of at least 50 nuclei are expressed as percentages of those in normal cells assayed in parallel. The error bars indicate SEM of three independent experiments.

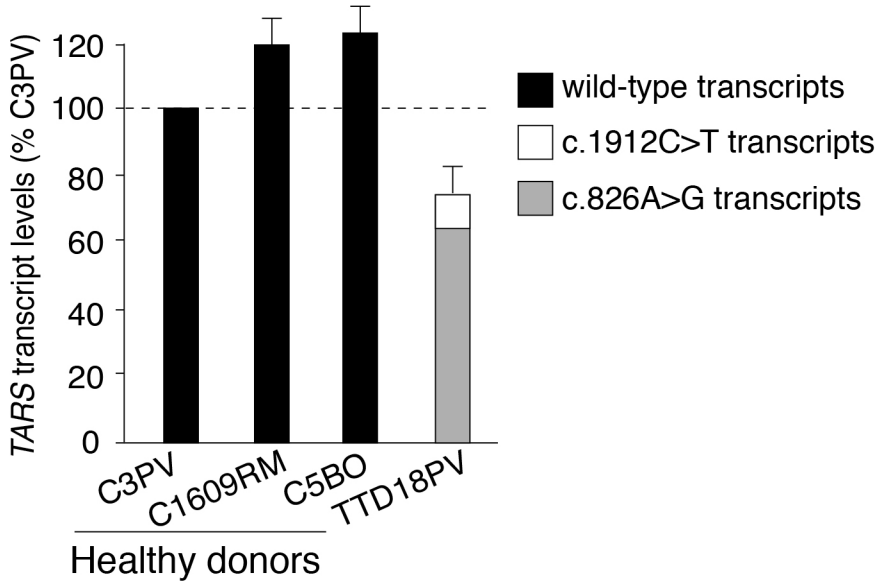

Figure S2. Analysis of mutant *TARS* transcript levels. Cellular levels of *TARS* mRNA assessed by qRT-PCR. Total TARS transcript levels were first normalized to the levels of *GAPDH* mRNA and then expressed as percentages of the corresponding value in the normal C3PV cells. The relative percentage of the mutant *TARS* transcripts in TTD18PV cells (c.1912C>T and c.826A>G) was assessed by allele-specific qRT-PCR. The reported values are the means of two independent experiments, each done in triplicate. The error bars indicate SEM.

Table S1: Hair analysis subject TTD18PV.

Aminoacid	**Normal Value**	**TTD18PV**
Aspartic acid	4,9	8,5
Threonine	6,9	3,0
Serine	10,8	10,1
Glutamic acid	11,4	16,8
Proline	9,0	8,6
Glycine	5,5	6,6
1/2 Cysteine	20,8	8,5
Valine	4,9	6,1
Methionine	0,3	0,2
Isoleucine	2,5	3,6
Leucine	6,0	9,1
Tyrosine	1,9	1,6
Phenylalanine	1,6	2,6
Histidine	0,9	1,1
Lysine	2,7	4,6
Arginine	5,0	6,5

Aminoacid content in the hair of the subject TTD18PV compared to a normal hair sample. Hair aminoacid content was determined using chromatography and values obtained for individual aminoacids were expressed as percentage.

Table S2. cDNA and genomic primers used in this study.

Assay[a]	Gene	Position[b]	Primer	Sequence 5'-3'
cDNA PCR	*TARS*	c.-9_-28	TARS_F1	GGTTCTCTCATCGCTTCGTC
		c.664_687	TARS_R1	CATTGCCAGTAAAGTTTCTTTCTT
		c.371_390	TARS_F2	ATGTTGTGTGGGACCTGGAC
		c.1167_1186	TARS_R2	TGTTCTCGCTGTAGTGCTGC
		c.970_989	TARS_F3	AGGAAAATTGGCAGGGACCA
		c.1771_1790	TARS_R3	ACTGATCCCAAGATGGCTCG
		c.1488_1507	TARS_F4	AAACCTTTCTACTCGCCCGG
		c.+11_+30	TARS_R4	TTCCATGGAGCCAATCTGGG
Genomic DNA PCR	*TARS*	16417_16436	TARS_int8F2	GGGGCATTTTTGAGGATAGA
		16764_16784	TARS_int9R2	TCATGCAGCTGAATTTCAAAC
		25989_26008	TARS_int18F2	AGAGGAGCTGGCCTTTTTGA
		26452_26473	TARS_int19R2	CCCAGTATGTATGCATGAGCCT
qRT-PCR	*TARS*	c.-73_-53	TARSv1_F1	CCTCTTGGCTCCTCTCCTCT
		c.320_339	TARSv1_R1	CAGGCCTTGACTAATTCCAC
		c.1763_1782	TARS_F1763	TTGTTCATCGAGCCATCTTG
		c.1912_1931	TARS_R1912G	GCATCGTGGAATTGTTG**G**C<u>G</u>
			TARS_R1912A	GCATCGTGGAATTGTTG**G**C<u>A</u>
	GAPDH	c.20_39	GAPDH_F2	GAGTCAACGGATTTGGTCGT
		c.204_185	GAPDH_R2	GACAAGCTTCCCGTTCTCAG

[a] PCR amplified cDNA and genomic DNA fragments were sequenced using the corresponding F and R PCR primers.

[b] Positions of cDNA PCR primers and qRT-PCR primers refer to the GenBank reference mRNA sequence NM_152295.4 (*TARS* variant 1, CDS 312-2483). For cDNA numbering, +1 corresponds to the A of the ATG translation initiation codon in the reference sequence. For primers TARS_R1912G and TARS_R1912A underlined nucleotides indicate wild-type and mutant nucleotides, respectively. In order to prevent the amplification of the non-matching primer, an additional nucleotide mismatch located three bases from the 3' termini was incorporated (indicated in bold).

Positions of genomic DNA primers refer to the *TARS* GenBank reference genomic sequence NC_000005.10 nt 33440696-33468091.

Supplemental Material and Methods

Whole genome sequencing (WGS)

Nanoball based massive parallel sequencing (software version 2.5.0.44) was done as described previously [1]. Image data analyses including base calling, DNB mapping, and sequence assembly. Reads were mapped to the National Center for Biotechnology Information (NCBI) reference genome, build 37. Variants were annotated using NCBI build 37 and dbSNP build 137. Data were provided as lists of sequence variants (SNPs and short indels) relative to the reference genome. Analysis of the massive parallel sequencing data was performed using Complete Genomics analysis tools (cga tools version 1.8.0 build 1; http://www.completegenomics.com/sequence-data/cgatools/) and TIBCO/Spotfire version 7.0.1 (http://spotfire.tibco.com/).

Whole exome sequencing (WES)

Exonic DNA was captured using the Agilent SureSelect Human All Exon target enrichment kit (Agilent Technologies, Santa Clara, CA) and sequencing was performed with paired-end 100bp reads on one-quarter of an Illumina Analyzer IIx (Illumina, San Diego, CA). About 50 M reads/individual were generated resulting in approximately 30-40x coverage of the targeted exome. The Genome Analysis Toolkit (GATK v2.5) was used to perform variant discovery and genotyping. SNPs and Indels were called according to the GATK's Best Practices. Variants were filtered assuming a recessive inheritance model. Given the rare incidence of TTD (estimated to be 1.2 per million livebirths in Western Europe [2]) only variants with a frequency ≤ 0.001 were considered. Variants prioritization was based on computationally predicted pathogenicity scores in SIFT and PolyPhen2.

Sanger validation sequencing

In TTD18PV the *TARS* mutation was confirmed in the relevant genomic DNA region based on WES findings. 24 additional TTD cases were screened for mutations in *TARS* by directed sequencing of either the cDNA or genomic DNA using PCR and sequencing primers (Table S2).

Quantitative RT-PCR

Total RNA was extracted using RNeasy Mini Kit (Qiagen, Hilden, Germany). Transcript levels of *TARS* and *GAPDH* (for normalization) were measured on a LightCycler 480 (Roche, Mannheim, Germany). Primer sequences are in Table S2.

Cell culture

Primary fibroblasts: TTD18PV (NPS-TTD), TTD5VI (NPS-TTD), C3PB, C1609RM, C5BO, C4RO and C5RO, were cultured in Ham's F10 medium (BE02-014F, Lonza) supplemented with 10% fetal bovine serum (S1810, Biowest) and 1% penicillin-streptomycin (P0781, Sigma-Aldrich) at 37°C, 20% O2 and 5% CO2.

Antibodies

Primary antibodies used: α-TARS (ab50795; Abcam), α-Tubulin (T5168, Sigma-Aldrich) and α-GFP (11814460001, Roche Diagnostics). Secondary antibodies used: CF680 anti-mouse (SAB4600199, Sigma-Aldrich), IRDye 800CW Donkey anti-mouse (926-32212,LI-COR) and Alexa Fluor 488 goat anti-mouse (A11001, Invitrogen).`

Colony forming ability/survival

Cells were plated in 10 cm dishes (1500 cells/dish), in triplicate. After 24 h, cells were irradiated with different doses of UV-C irradiation (0-8 J/m^2) and incubated for approximately 2 weeks. Colonies were fixed and stained with 0.1% Brilliant Blue R (Sigma) and counted (Gelcount, Oxford Optronix Ltd.). The survival was plotted as the percentage of colonies obtained after treatment compared to the mean number of colonies from the mock-treated cells (set at 100%).

Unscheduled DNA synthesis (UDS) assay

For UDS, GFP (Green Fluorescent protein)-expressing control fibroblasts were mixed with fibroblasts from subject TTD5VI, subject TTD18PV, a healthy individual (C5RO) or a DNA repair deficient subject (XP-A), and seeded onto 24 mm cover slips. Two days later adherent cells were washed with PBS and UV-C irradiated with 16 J/m^2. Thereafter, fibroblasts were incubated for 3 h in medium containing 0.1 µM 5-ethynyl-2'-deoxyuridine (EdU, A10044, Invitrogen). After EdU incorporation, fibroblasts were fixed in 2% formaldehyde/PBS, washed with 3% BSA/PBS, permeabilized for 20 min in 0.1% Triton/PBS and washed once with PBS. Samples were incubated for 30 min with fluorescent dye coupling buffer containing 10 mM CuSO4 and Atto 594 azide (AD 594-105, ATTO-TEC), washed with 0.1% Triton X-100/PBS, rinsed for 15 min in PBS+ (PBS containing 0.15% glycine and 1% BSA). For visualizing GFP-expressing cells, samples were incubated for 2 h with monoclonal GFP antibody diluted in PBS/Triton X-100 in a moist chamber, washed with PBS+ and incubated for 1 h with secondary antibodies diluted in PBS/Triton X-100 at room temperature in moist chamber. After washing in PBS/Triton X-100 samples were embedded in Vectashield mounting medium with DAPI (H-1200, Vector Laboratories). UDS levels were expressed as

the average fluorescence intensity in the nucleus of subject fibroblasts versus GFP-expressing control fibroblasts, which was set at 100%. The mean fluorescence is determined with a confocal microscope (Zeiss LSM 700) from at least 50 cells and three independent experiments. Images were processed using ImageJ.

Immuno-blot analysis

Whole cell extracts were isolated as follows: cells were washed with PBS and directly lysed in SDS-PAGE Laemmli sample buffer, separated on a Mini-PROTEAN TGX Gel (#456-1084, BIO-RAD), blotted onto Immobilon-FL membrane (IPFL00010, Merck Millipore Ltd.), stained with specific primary and secondary antibodies and analyzed using an Odyssey imager (LI-COR). Immunoblots were quantified using ImageStudio Lite (ver. 5.2, LI-COR Biosciences).

Yeast Complementation Assays

Complementation assays were performed by plasmid shuffling experiments. Briefly, yeast cells (haploid *S. cerevisiae* BY4743 ths1- strain harbouring a pRS426 maintenance vector expressing the wild-type yeast *THS1* and *URA3*) were transformed with *LEU2* pRS425 vectors expressing either wild-type or mutated human *TARS* cDNA and then the yeast strain was grown in selective medium lacking leucine and uracil (-LU) to select for the presence of both vectors. Next, the cells were spotted on plates containing 0.1% 5-Floroorotic acid (5-FOA) or -LU medium and incubated at 30°C for 96 hours. 5-FOA is toxic to yeast cells expressing URA3 and thus select for cells that have spontaneously lost the maintenance vector. Only those cells containing a functional gene expressed from the LEU2 plasmid are

able to complement the cell lethality caused by the deletion of endogenous gene and survive on 5-FOA plates. Survival was determined by visual inspection of growth.

Aminoacylation reaction

Assays were performed at 37°C in reaction buffer (50 mM Tris buffer pH 7.5, 12 mM MgCl , 25 mM KCl, 1 mg/mL bovine serum albumin, 0.5 mM spermine, 1 mM ATP, 0.2 mM yeast total tRNA, 1 mM dithiotreitol, 0.3 mM [$^{13}C_4$,^{15}N] threonine and [D_4] lysine. The aminoacylation reaction was terminated by adding trichloroacetic acid (TCA) and subsequently washed. Ammonia was added in order to release [$^{13}C_4$,^{15}N] threonine and [D_4] lysine from the charged tRNAs. [D_2] glycine and [$^{13}C_6$] arginine were added as internal standards. Labeled amino acids were quantified by liquid chromatography-tandem mass spectrometry (LC-MS/MS).

Supplemental References

1. Drmanac, R., Sparks, A.B., Callow, M.J., Halpern, A.L., Burns, N.L., Kermani, B.G., Carnevali, P., Nazarenko, I., Nilsen, G.B., Yeung, G., et al. (2010). Human genome sequencing using unchained base reads on self-assembling DNA nanoarrays. Science 327, 78-81.
2. Kleijer, W.J., Laugel, V., Berneburg, M., Nardo, T., Fawcett, H., Gratchev, A., Jaspers, N.G., Sarasin, A., Stefanini, M., and Lehmann, A.R. (2008). Incidence of DNA repair deficiency disorders in western Europe: Xeroderma pigmentosum, Cockayne syndrome and trichothiodystrophy. DNA Repair (Amst) 7, 744-750.